Portable Nano-Particle Emission Measurement System

EUROPEAN COMMISSION
Horizon 2020 | GV-02-2016 | Technologies for low emission light duty powertrains
GA # 724145

Deliverable No.	PEMs4Nano D2.10	
Deliverable Title	Report on particle losses in the instruments	
Deliverable Date	2019-12-31	
Deliverable Type	REPORT	
Dissemination level	Public (PU)	
Written By	Philipp Kreutziger (HORIBA Europe GmbH)	2019-12-10
Checked by	Torsten Tritscher (TSI GmbH)	2019-12-18
Approved by	Juergen Spielvogel (TSI GmbH) Pascale Desgroux (ULL) Jethro Akroyd (UCAM) Marcus Rieker (HORIBA) - Coordinator	2019-12-18 2019-12-18 2019-12-18 2019-12-19
Status	Final Report	2019-12-19

Publishable Executive Summary

This report describes the investigation of particle losses in the 10 nm PEMS prototype. The results of the prototype testing, calibration and optimization are presented. The particle losses and measurement efficiency of the new system are quantified on the basis of data acquired using an existing reliable and accurate calibration test bench. Experimental and modelling investigations are performed to assess the methods used to calculate the particle losses occurring due to particle diffusion in the sample and transport lines (between the source of emissions and the PEMS instrument). Initial recommendations are made.

Contents

Figures

Tables

1 Introduction

The overall goal of the PEMs4Nano project is to develop robust and reliable measurement procedures for particulate emissions from 10 nm upwards in size, and to provide a contribution to future regulation on particle emissions for current gasoline direct injection (GDI) internal combustion (IC) engines. The project includes developing a fundamental understanding of the particle formation and loss mechanisms, starting from the formation of particles in the engine, through the exhaust system and during sampling as the emissions are drawn into the measurement device. In addition, it is necessary to understand the particle transport mechanisms to identify the most important loss functions and parameters that affect the measurement of the particulate emissions.

The particle losses in the PEMS device developed during the project have been theoretically calculated and characterized experimentally. The experiments make use of the calibration test bench to perform reliable and accurate measurements of the particle losses and system efficiency (corresponding to D2.07). The experimental characterization is supported by experiments performed at the University of Lille (ULL) and analysis performed independently at the University of Lille (ULL) and the University of Cambridge (UCAM) to investigate the ability to accurately model the diffusional losses of particles that occur in transfer lines.

2 Calculation of particle losses and penetration efficiency

The following section describes the methods used to calculate particle losses. The methods are well-established and documented in the scientific literature [1].

2.1 Sources of particle transformation and losses

In order to evaluate the quantitative particle losses inside a sub-23nm measurement device it is necessary to understand all the possible loss mechanisms inside the instrument. The main loss mechanisms are [1]:

- Diffusion
- Electrophoresis
- Thermophoresis
- Agglomeration
- Evaporation
- Impaction
- Sedimentation

The particle loss mechanisms can be divided into two different groups. The first group describes internal processes (Figure 2-1). When the number density of the particles is high (i.e. there is a large number of particles in a small volume), these internal losses are mainly dominated by agglomeration [2]. Given the significant dilution of the exhaust sample before it enters the measurement device, the internal losses are assumed to be negligible. Evaporation belongs also to the internal losses but is not relevant for the device since only solid particles will be counted in the end.

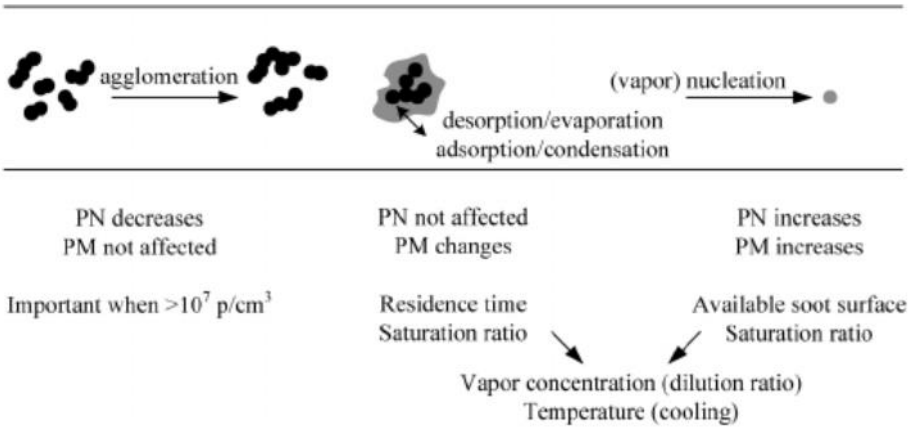

Figure 2-1 Particle dynamics and transformation (internal processes) [2].

The focus within this report is therefore on the second group, known as external processes (Figure 2-2) [2]. Sedimentation or gravitational losses are only relevant for very large particles and therefore identical in 23 nm and sub-23 nm systems and not of importance. The use of electrically conductive material in all aerosol-carrying lines and sections minimizes any potential electrostatic loss. Very small particles have a high mobility. When small particles are transported through tubing and components, size dependent diffusion losses can be significant. The primary loss mechanisms considered in this report are therefore diffusion due to Brownian motion of the particles in air and inertial impaction due to bends. By careful dilution and cooling, thermophoretic losses can be reduced significantly.

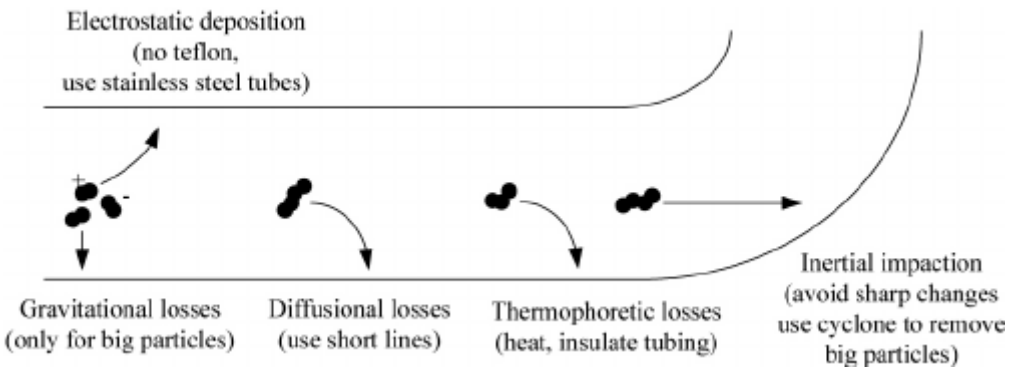

Figure 2-2 Mechanisms of particle losses (external processes) [2].

2.2 General Calculation Methodology

The penetration efficiency (η) is defined as the ratio of downstream number concentration to upstream concentration [3]. In case of transport in bends, the total efficiency η_{all} is the product of the particle penetration efficiency due to diffusion η_{diff} and due to inertial transport in bends η_{bends}.

Theoretical particle penetration efficiencies may be calculated according to the following equation:

$$\eta_{all} = \eta_{diff} \cdot \eta_{bends} \quad [-] \qquad \text{Eq. 2-1}$$

where η_{diff} and η_{bends} are the particle penetration efficiencies resulting from losses due to diffusion and due to inertial impaction in bends. The equations are well-established and are explained in detail in the following paragraphs [4].

a) Diffusional deposition

Particle diffusion penetration efficiency for a laminar flow in a pipe was calculated via the following set of equations:

$$\eta_{diff} = \exp(-\xi Sh) \quad [-] \qquad \text{Eq. 2-2}$$

with,

$$\xi = \frac{\pi D_{diff} L}{Q} \quad [-] \qquad \text{Eq. 2-3}$$

and

$$Sh = 3.66 + \frac{0.2672}{\xi + 0.10079\xi^{1/3}} \quad [-] \qquad \text{Eq. 2-4}$$

where D_{diff} is the particle size specific diffusion coefficient in [m^2/s], L is the tube length in [m], Q is the volumetric flow of the medium in [m^3/s] and Sh is the dimensionless Sherwood number. The particle diffusion coefficient, a parameter for the strength of the diffusion effect, was calculated according to the following equation:

$$D_{diff} = \frac{k_B T C_c}{3\pi\mu d_{ma}} \quad [m^2/s] \qquad \text{Eq. 2-5}$$

with,

$$Cc = Cc_1 + K_n\left(C_{c2} + C_{c3}\exp(-C_{c4}/K_n)\right) \quad [-] \qquad \text{Eq. 2-6}$$

$$K_n = \frac{2\lambda}{d_{ma}} \quad [-] \qquad \text{Eq. 2-7}$$

$$\lambda = \frac{\mu}{P}\sqrt{\frac{\pi R_g T}{2M}} \quad [m] \qquad \text{Eq. 2-8}$$

$$\mu = \frac{A_1}{T + A_2} T^{1.5} \quad [Pa\ s] \qquad \text{Eq. 2-9}$$

where, k_B is the Boltzmann constant, C_c is the Cunningham correction factor, μ is the viscosity of the flowing medium, d_{ma} is the aerodynamic particle diameter, K_n is the Knudsen number, λ is the free mean path of the particles in the flowing medium, P is the pressure, T is the temperature, R_g is the universal gas constant and M is the mean molar weight of the medium molecules.

The carrier gas transport data were approximated as those of pure N_2. The Cunningham correction factor constants and constants in Sutherland's viscosity formula are presented in Table 2-1.

Table 2-1 Carrier gas transport data.

Carrier gas	M [kg/mol]	C_{c1} [-]	C_{c2} [-]	C_{c3} [-]	C_{c4} [-]	A_1 [K]	A_2 [Pa s $K^{-1.5}$]
N_2	0.028	1.0	1.246	0.42	0.87	111.0	1.406732×10^{-6}

The particle aerodynamic diameter was calculated as follows:

$$d_{ma} = d_m\sqrt{\frac{\rho_s}{\rho_0}} \quad [nm] \qquad \text{Eq. 2-10}$$

where, ρ_s is the soot density taken equal to 1.8 g/cm3 (as defined in Table 4-2 and Table 4-4) and ρ_0 is the unit density equal to 1.0 [g/cm^3] [4].

b) Inertial impaction deposition in bends

The particle penetration efficiency for a laminar flow in a pipe with bends was calculated according to the following formula:

$$\eta_{bends} = \left(1 + \left(\frac{Stk}{0.171}\right)^{0.452\frac{Stk}{0.171}+2.242}\right)^{-\frac{2}{\pi}\varphi} \quad [-] \qquad \text{Eq. 2-11}$$

with,

$$\mathrm{Stk} = \frac{\tau u}{d_{in}} \ [-] \qquad \text{Eq. 2-12}$$

$$\tau = \frac{d_{ma}^2 \rho_s C_c}{18\mu} \ [s] \qquad \text{Eq. 2-13}$$

where, φ is the overall bend angle in radians, Stk is the dimensionless Stokes number and τ is the particle relaxation time.

2.3 Calculation of penetration efficiency of the PEMs4Nano instruments

The loss calculations in the PEMS4Nano instruments were performed using a dimensionless deposition parameter

$$\mu = \frac{\xi}{\pi} \qquad \text{Eq. 2-14}$$

where ξ is defined as per Eq. 2-3. The corresponding penetration efficiency (i.e. the proportion of particles that are not lost), P, is calculated using the following relations [1]:

$$\text{for } \mu < 0.009 \qquad \eta = 1 - 5.50\mu^{2/3} + 3.77\mu \qquad \text{Eq. 2-15}$$

$$\text{for } \mu > 0.009 \qquad \eta = 0.819e^{(-11.5\mu)} + 0.0975e^{(-70.1\mu)} \qquad \text{Eq. 2-16}$$

where the choice of whether to use equation 2-15 or 2-16 depends on the magnitude of the dimensionless deposition parameter, μ.

3 Characterization of PEMS devices

The goal of the project is to develop robust and reliable measurement technology with a threshold detection size of at least 10 nm (i.e. the threshold detection size must be less than or equal to 10 nm). Therefore, the diffusional losses have been calculated assuming 10 nm particles [1]. In order to do this, the equipment was divided into 11 sections, where the losses in each section were calculated separately. The sections are shown in Figure 3-1. On the basis of the calculations, the design of each section of the instrument was optimized to minimize the losses.

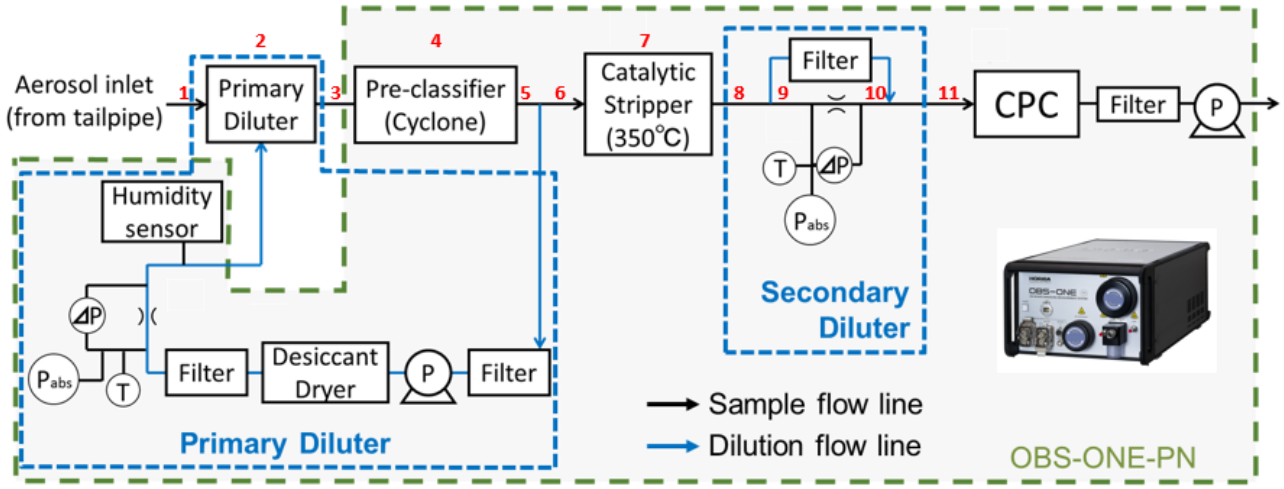

Figure 3-1 Schematic of the PEMS prototype for sub-23nm particle number measurement [5].

The diffusion in each section was calculated as per Section 2.3. The overall penetration efficiency is calculated as the product of the penetration through each individual section. The calulation predicts an overall penetration efficiency of approximately 67% for 10 nm particles when considering a 2.5 m heated sample line (HSL).

3.1 Comparison between calculation and measurement on particle losses inside the PEMS

3.1.1 Overall Instrument (System efficiency)

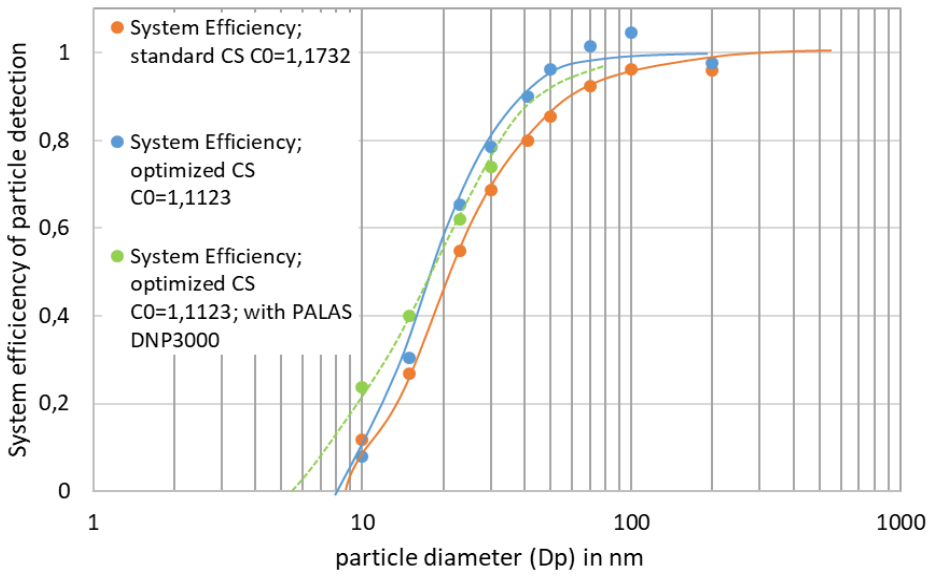

Figure 3-2 PEMs4Nano PEMS - Experimental system efficiency with original and optimized CS for cast and spark-generated soot [5].

Figure 3-2 shows the experimentally determined particle detection efficiency of the PEMs4Nano instrument at different stages of optimization. The experimental data with the optimized CPC show a system efficiency of around 10% at 10 nm (orange line) for thermally conditioned flame cast soot. Note that the experimental value of 10% includes a correction factor of 1.1732 to ensure 100% detection efficiency at 200 nm, such that the uncorrected system efficiency is less than 10%. It should also be noted that only 52% of 10 nm particles are detected by the optimized CPC (see Report D2.07 Figure 3-4). If the CPC would detect 100% of 10 nm particles, this would lead to a system efficiency (i.e. something directly comparable to the calculation, which does not consider the counting efficiency of the CPC) of around 20%. In all cases, the experimental data show a considerable discrepancy with the calculated value of approximately 67% for 10 nm particles.

Looking at the measurement at 10 nm with thermally conditioned flame cast soot (blue line) and with spark-generated soot (green line), the penetration efficiency is between 10% and 25% respectively. A correction factor of 1.1123 has been applied to achieve 100% detection efficiency of 200 nm particles.

The same consideration must be taken, that only 52% of 10 nm particles are detected by the CPC, so it would be possible to detect up to 45% of 10 nm particles if the CPC detects 100% of particles at 10nm. This value is still far below the previously calculated value of 67% for the whole system.

3.1.2 Penetration Efficiency of Catalytic Stripper

The catalytic stripper (CS) is the sub-system that has the main impact on the overall penetration efficiency. Given this and the high operating temperature of the catalytic stripper, 350°C, where it is known that diffusional losses will increase with temperature), it was decided to optimize the catalytic stripper to improve particle penetration.

Figure 3-3 shows experimental measurements of the penetration efficiency through the catalytic stripper measured using silver particles. The left-hand panel shows data for the unoptimized catalytic stripper. The right-hand panel shows data for the optimized catalytic stripper. The data for the penetration efficiency of 10 nm particles in unoptimized catalytic stripper (left-hand panel) shows a far lower efficiency than the calculated value (even without scaling the data in Figure 3-3 to the 0.7 SLPM used in the catalytic stripper in the PEMs4Nano instrument). In the optimized catalytic stripper (right-hand panel), the experimental data at 0.75 SLPM, 350°C show a penetration efficiency of approximately 65% for 10 nm particles. This is still less than the calculated value. At 25°C the measured penetration efficiency increases to 80%, so still less than the calculated value. The reason for the temperature dependence cannot be assigned to one specific loss mechanism. It could be possible that thermophoretically losses in addition to diffusional losses are the dominating mechanism inside the catalytic stripper. More evaluation is necessary in the future to determine the influences.

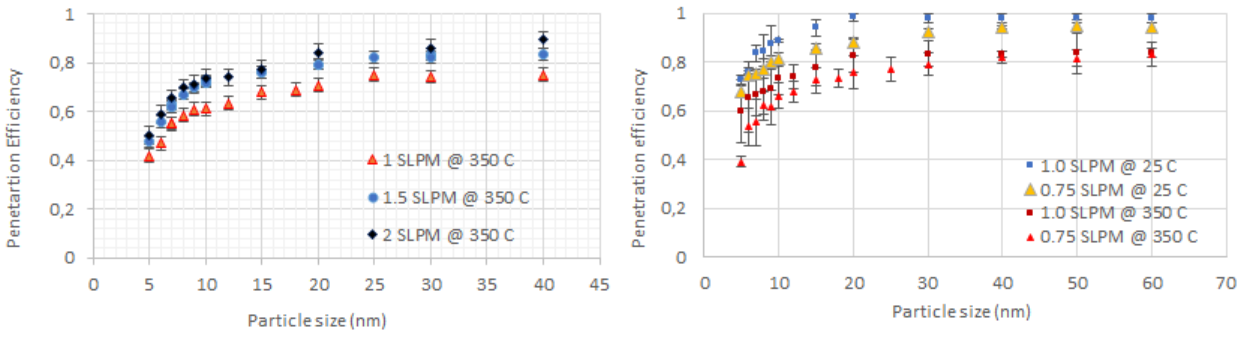

Figure 3-3 Solid particle penetration efficiency through catalytic stripper (left, original CS; right, optimized CS) [4].

The experimental data shows that the overall performance of the catalytic stripper is good, and that the PEMS device can be used to measure particles down to 10 nm in size. However, the ability to calculate the losses was much worse than expected, particularly given that the calculations were performed using established textbook-standard equations. For this reason, further experimental investigations were undertaken to investigate the discrepancy.

4 Fundamental studies of particle losses

The particles losses through tubes of different lengths were measured in carefully controlled laboratory experiments. The corresponding particle losses were estimated under the assumption that the losses were dominated by diffusion, and the results critically assessed.

4.1 Determination of particle losses

Experiments have been set-up in order to measure the losses undergone by carbonaceous particles in standard sampling tubes of 5.2 mm inner diameter. The set-up consists of a particle generator connected to a Scanning Mobility Particle Sizer (SMPS) spectrometer for measuring the particle number size distribution. Between the generator and the SMPS, various lengths of tube or and flow rates were investigated, Fig. 4-1:

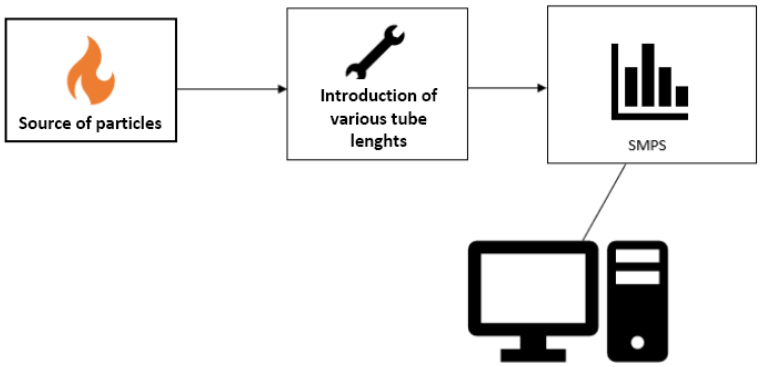

Figure 4-1 Set-up implemented for losses measurements.

Two particles generators were used to scan the size range from 2 nm to 100 nm:
1) Set-up A: Generation of nano-scale graphite aerosols using a PALAS DNP 2000 spark generator. The particle size distribution was centered on 44 nm and measured with a SMPS (TSI 3936L76 with classifier 3080, long DMA 3081 and CPC 3776), see Figure 4-2:

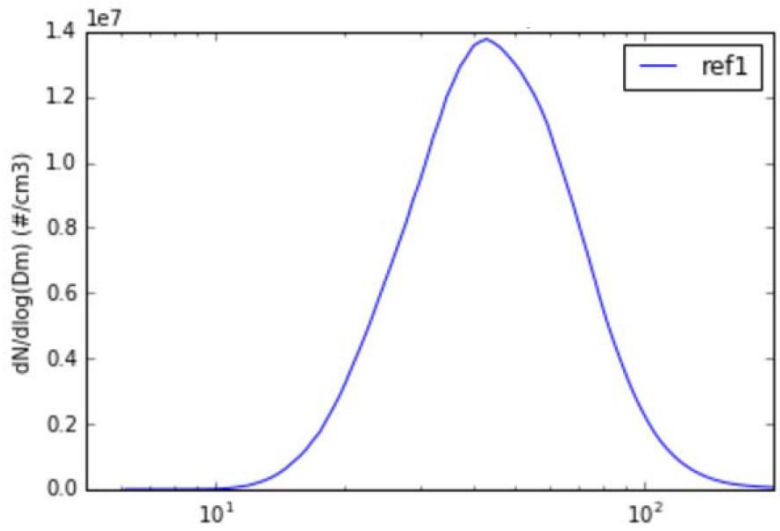

Figure 4-2 Size distribution (nm) of graphite particles generated by the PALAS spark generator.

2) Set-up B: Generation of soot particles in an atmospheric premixed methane/oxygen/nitrogen-flame stabilized on a Holthuis burner. The particle size distribution is bimodal and well below 10 nm with a mode centered at 2.84 nm and a second centered at 6.8 nm. The measurement was performed with a 1 nm SMPS (TSI 3938E57 with Classifier 3082, DMA 3086 and CPC 3750 + Nanoenhancer 3757), see Figure 4-3:

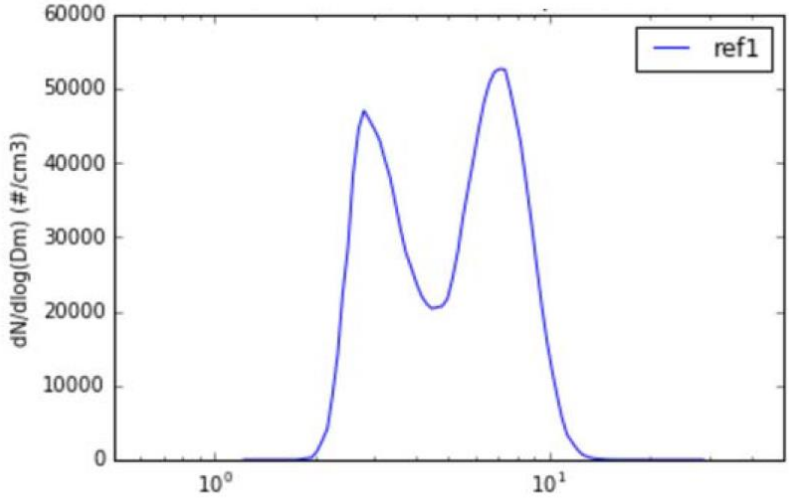

Figure 4-3 Bimodal size distribution (nm) of soot particles produced in a premixed flame.

The dilution flow rate was high enough to prevent coagulation in the sampling tubes. The shape of the size distributions was shown to be unchanged (from 10 to 100 nm for PALAS particles and from 2 to 10 nm for burner soot particles) in mode position (peak) and geometrical standard deviation when longer tubes or varying flow rates were used. Therefore, for each experiment, only the losses at the distribution mode D_m is reported.

4.2 Independent calculation of particle losses

Additional independent calculations were performed to double check the analysis of the results for each of the experiments described in Section 4.1. The overall particle losses due to diffusion and inertial particle deposition were calculated for the desired conditions. To verify the impact on the calculation and measurement results according to the temperature, a sensitivity analysis was performed in order to test the model response.

5 Conclusions

The particle losses in the PEMS device have been characterized experimentally, and each component within the PEMS device optimized to minimize losses. The component responsible for the largest proportion of the losses, and therefore subject to most of the optimization effort, was the catalytic stripper. The experimentally characterized losses in the optimized device have been demonstrated to be acceptable for use of the PEMS device to measure emissions of solid particles down to 10 nm in size.

Additional fundamental experiments were performed to understand the loss processes because it was observed that calculations of the expected losses underestimated the experimentally observed particle losses inside the PEMS device. Possible reasons for this underestimation in the device might be:

- Shapes / Diameter changes of the individual components
- Material changes in example from stainless steel to conductive tubing
- Local turbulence effects (even though the overall flow is laminar)
- Charging effects and electrostatic losses due to the relatively highly charged spark-generated soot.

The additional experiments focused on diffusional losses, which are the basis of most of the loss calculations performed for the PEMS device. The results of the experiments need to be further evaluated. It is suggested that the future experiments should, if possible, seek to use a simpler geometry and should simultaneously measure the particle number densities before and after the tube. This would require two instruments.

6 Recommendations

The particle losses in the instrument have been investigated. The ability of well-established calculation methods to predict the diffusion losses in an instrument underpredict the experimental losses. The following recommendations are made:

- The PEMS device developed during the project has undergone rigorous experimental testing; the particle losses in the equipment have been characterized experimentally and the PEMS device has shown to be able to measure emissions of particles that are 10 nm or larger in size.
- Further scientific investigation is necessary to understand particle loss mechanisms

7 Deviations from Annex 1

There are three deviations:

1. Originally TSI was responsible for writing D2.10, and Horiba was reviewer. At the 7th General Assembly in Mülheim an der Mosel (Germany) it was decided that Horiba writes this deliverable instead of TSI, because it fits better with the expertise. TSI has reviewed the deliverable.
2. D2.10 includes results that were obtained using the 2nd PEMS. This 2nd PEMS was available thanks to the budget shift in 2018 that was approved by the project officer on November 14th 2018, and that is described in the Period 2 report under Deviations.
3. The public version of D2.10 contains a higher-level description of the technical details and is submitted in the Participant Portal. A confidential version with all full technical details was sent directly to the project officer.

8 Acknowledgement

The author(s) would like to thank the partners in the project for their valuable comments on previous drafts and for performing the review.

Project partners:

#	Type	Partner	Partner Full Name
1	IND	HORIBA	Horiba Europe GmbH
2	IND	Bosch	Robert Bosch GmbH
3	IND/SME	CMCL	Computational Modelling Cambridge Limited
4	IND	TSI	TSI GmbH
5	HE	UCAM	The Chancellor, Masters and scholars of the University of Cambridge
6	HE	ULL	Université des Sciences et Technologies De Lille – Lille I
7	IND	IDIADA	Idiada Automotive Technologie SA
8	IND	HORJY	Horiba Jobin Yvon S.A.S.
9	IND/SME	UNR	Uniresearch BV

This project has received funding from the European Union's Horizon2020 research and innovation programme under Grant Agreement no. 724145.

9 References

[1] William C. Hinds, Aerosol Technology – Properties, Behavior and Measurement of Airborne Particles Second Edition, John Wiley and Sons Inc., 1999
[2] Giechaskiel et al., SAE Int. J. Engines, Volume 5, Issue 2, May 2012
[3] Yook et al. AST 2006, vol 40, pp 456-462
[4] J. E. Brockmann, “Chapter 6: Aerosol Transport in Sampling Lines and Inlets,” in Aerosol Measurement, John Wiley & Sons, Ltd, 2011.
[5] PEMs4Nano report D2.07

Appendix A – Abbreviations / Nomenclature

Table B-1 List of Abbreviations / Nomenclature.

Symbol / short name	
C0-factor	Dimensionless particle concentration reduction factor for PEMS
CH4	Methane
CPC	Condensation Particle Counter
CS	Catalytic Stripper
DMA	Differential Mobility Analyzer
Dp	Particle Diameter
GDI	Gasoline Direct Injection
HSL	Heated Sample Line
H2	Hydrogen
IC	Internal Combustion
PEMS	Portable Emission Measurement System
SMPS	Scanning Mobility Particle Sizer
SLPM	Standard Liters Per Minute
UCAM	University of Cambridge
ULL	University of Lille